Ion–Amide Interactions

International Edition: DOI: 10.1002/anie.201602769
German Edition: DOI: 10.1002/ange.201602769

# Dissecting Hofmeister Effects: Direct Anion–Amide Interactions Are Weaker than Cation–Amide Binding

*Vasileios Balos, Heejae Kim, Mischa Bonn, and Johannes Hunger**

***Abstract:*** *Whereas there is increasing evidence for ion-induced protein destabilization through direct ion–protein interactions, the strength of the binding of anions to proteins relative to cation–protein binding has remained elusive. In this work, the rotational mobility of a model amide in aqueous solution was used as a reporter for the interactions of different anions with the amide group. Protein-stabilizing salts such as KCl and $KNO_3$ do not affect the rotational mobility of the amide. Conversely, protein denaturants such as KSCN and KI markedly reduce the orientational freedom of the amide group. Thus these results provide evidence for a direct denaturation mechanism through ion–protein interactions. Comparing the present findings with results for cations shows that in contrast to common belief, anion–amide binding is weaker than cation–amide binding.*

The effect of salts on biomolecular behavior, such as protein denaturation, protein crystallization, and enzymatic activity, has been proven to follow the Hofmeister series,[1–5] which states that cations with a high surface charge density and anions with a low surface charge density tend to destabilize proteins. In recent years, it has been manifested that direct interactions between biomolecules and ions dominate these effects,[2,3] although water-mediated, indirect effects are also not negligible.[4,6,7] The direct interactions between biomolecules and ions are highly complex[3,5] because of 1) the complexity of the salt solutions themselves[8] and 2) the plethora of potential specific and non-specific interaction sites of biomolecules (e.g., the backbone, side chains, and termini of a protein).[3,4,9,10] Owing to this complexity, it is imperative to correlate the binding of ions to biomolecules with Hofmeister effects to gain a detailed understanding of the underlying mechanism.[3]

Direct interactions between ions and the amide backbone, the structural motif common to all proteins, have been studied by numerous spectroscopic studies.[9,11–14] Although direct interactions are occasionally challenged,[15] studies of the NMR chemical shifts of the amide protons[9,11,12] showed that the proximity of an anion to an amide follows the Hofmeister series.[16] Likewise, the amide C=O vibration[14] and also the NMR chemical shift of the C=O carbon atom[17] are affected by interactions with cations, in line with direct amide–cation binding.[14] These studies have led to the view that cation–amide interactions play a less important role in Hofmeister effects than anion–amide interactions.[3,14] However, whereas some computational studies support this view,[12,16,18] others have reached the opposite conclusion.[19] The different spectroscopic sensitivities and/or the different interaction sites that have been studied (e.g., the N–H or the C=O group of the amide) make it nearly impossible to compare the interaction strengths of cations and anions. Herein, we use the rotational mobility of an amide group as a measure for ion–amide interactions[20] as it is equally sensitive to interactions with both cations and anions.

To study the anion–amide interaction, we used aqueous solutions of *N*-methylacetamide (NMA) in the presence of inorganic salts. Although NMA and its rotational dynamics differ from a protein, it is an ideal model to exclusively study the interactions specific to the amide group. To study a wide range of monovalent anions within the Hofmeister series, we added the potassium salts of $Cl^-$, $NO_3^-$, $Br^-$, $I^-$, and $SCN^-$. While the concentration of the salts, $c_{salt}$, was varied, the concentration of NMA was kept constant at $2\,mol\,L^{-1}$. The rotational dynamics of NMA in solution were determined by dielectric relaxation spectroscopy (DRS), which probes the polarization of the samples in an externally applied alternating electric field with a field frequency $\nu$.[21,22] For dipolar liquids at microwave frequencies, the polarization predominantly results from the alignment of the permanent dipoles along the applied electric field. For the present samples, DRS thus probes the rotation of both dipolar water and dipolar NMA molecules. The frequency-dependent polarization is measured as the complex permittivity, $\hat{\varepsilon}(\nu) = \varepsilon'(\nu) - i\varepsilon''(\nu)$, with the real part $\varepsilon'(\nu)$ representing the permittivity and the imaginary part $\varepsilon''(\nu)$ the dielectric loss. Here, we covered frequencies of $0.8 \le \nu/\mathrm{GHz} \le 36$ and $56 \le \nu/\mathrm{GHz} \le 125$ using a frequency domain reflectometer and $0.3 \le \nu/\mathrm{THz} \le 1.6$ using a THz time-domain spectrometer (for details see the Supporting Information).[23]

In Figure 1, the dielectric spectra of aqueous NMA solutions ($2\,mol\,L^{-1}$) with varying concentrations of KI are shown. All spectra are dominated by a dispersion in $\varepsilon'$ centered at approximately 10 GHz and a corresponding peak in $\varepsilon''$. This relaxation stems from the orientational relaxation of the dipolar water and NMA molecules, with both relaxations strongly overlapping.[20,24] As apparent from Figure 1, the dominant effect of adding electrolyte to the solution is a reduction of the total relaxation amplitude, that is, a decrease in the (loss) peak area. The decrease in the relaxation amplitude is accompanied by a reduction of the static dielectric constant (the limiting value of $\varepsilon'$ for $\nu \to 0$).

[*] V. Balos, Dr. H. Kim, Prof. M. Bonn, Dr. J. Hunger
Department for Molecular Spectroscopy
Max Planck Institute for Polymer Research
Ackermannweg 10, 55128 Mainz (Germany)
E-mail: hunger@mpip-mainz.mpg.de
Supporting information and the ORCID identification number for an author of this article can be found under http://dx.doi.org/10.1002/anie.201602769.

  

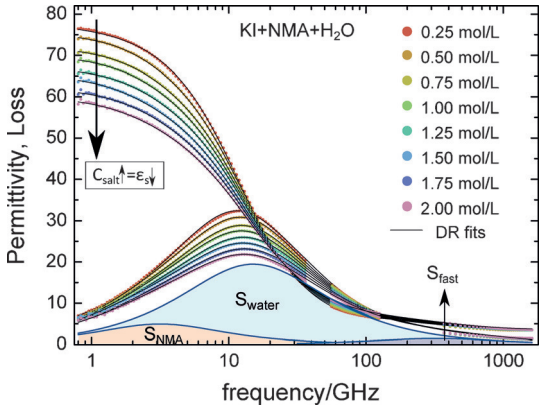


***Figure 1.*** Complex permittivity spectra of NMA(aq) with increasing KI concentration. Symbols correspond to experimental data, and solid lines show fits obtained with the dielectric relaxation model [Eq. (1)]. The shaded areas show the contributions of the individual relaxation modes to $\varepsilon''(\nu)$ for $c_{salt}$ =2 mol L$^{-1}$ (red: NMA; light blue: bulk water; dark blue: fast water relaxation). The Ohmic loss contribution [the last term of Eq. (1)] has been subtracted for visual clarity.

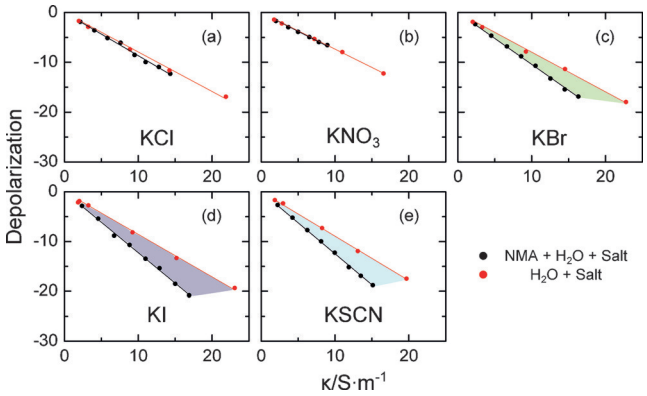


***Figure 2.*** Total depolarizations, $\Delta\varepsilon$, for a) KCl, b) $KNO_3$, c) KBr, d) KI, and e) KSCN in aqueous (red) and aqueous NMA (2 mol L$^{-1}$) solutions (black), as a function of the conductivity, $\kappa$. The shaded areas are visual aids to highlight the differences between solutions with and without NMA.

This decrease in permittivity, given by $\Delta\varepsilon = \varepsilon'_{\nu\to0}(c_{salt}=0) - \varepsilon'_{\nu\to0}(c_{salt}))$, is generally referred to as depolarization and is common to all studied samples (see the Supporting Information, Figures S1 and S2).

In general, the magnitude of the dielectric constant is determined by the equilibrium alignment of the molecular dipoles against thermal motion. Thus depolarization is indicative of a reduced ability of the dipoles to align to the external field. For the present samples, a minor contribution to the depolarization stems from the dilution of the molecular dipoles upon salt addition ($c_{H_2O}$ is reduced upon increasing $c_{salt}$). For electrolyte solutions, $\Delta\varepsilon$ is correlated to the presence of mobile ions and scales with the conductivity of the sample, $\kappa$,[20,25,26] which is in line with kinetic depolarization (KD)[20,25–27] being the dominating depolarization mechanism. KD results from the coupling of the translational motion of the ions to the rotational motion of the dipolar molecule: The molecular dipoles follow the strong local electrical field imposed by a passing ion rather than the externally applied electric field. It is important to note that for the ternary mixtures used here—as a result of the large effective dipole moment of NMA and the sensitivity of DRS to the squared dipole moment—$\Delta\varepsilon$ is about five times larger when ions affect a NMA molecule than the reduction of the rotational mobility of a water molecule.[20] Thus the magnitude of $\Delta\varepsilon$ with varying $\kappa$ for aqueous solutions of NMA and salt provides insight into the distribution of ions within the solution: With increasing proximity of the ions to the NMA molecules in solution, the magnitude of $\Delta\varepsilon$ will increase. The depolarization of the aqueous salt solution represents the limiting case where the ions solely affect the water molecules. Hence, comparing $\Delta\varepsilon$ values for NMA/salt/$H_2O$ solutions to $\Delta\varepsilon$ values for salt/$H_2O$ solutions provides a direct measure of the ion–NMA interaction strength.

In Figure 2, the measured $\Delta\varepsilon$ values as a function of $\kappa$ for the studied salts of the Hofmeister series both in aqueous solution (red symbols) and for solutions containing 2 mol L$^{-1}$ NMA (black symbols) are shown. The slopes shown in Figure 2 for the salt/$H_2O$ solutions are nearly independent of the nature of the salt (except for $KNO_3$ and KSCN where ion–pair relaxation and anion relaxation, respectively, contribute;[28] see the Supporting Information), which indicates that the observed depolarization can be qualitatively accounted for by dilution and KD as the underlying depolarization mechanism (Figure S3). This observation is in agreement with earlier studies of aqueous solutions of these ions.[29,30] In contrast to the binary salt/$H_2O$ samples, the slope of the depolarization versus $\kappa$ for the ternary solutions (NMA/salt/$H_2O$) strongly depends on the nature of the anion: Whereas for ions with a weak protein denaturation tendency such as KCl and $KNO_3$ the data for the aqueous solution and for the 2 mol L$^{-1}$ NMA solution virtually overlap (Figure 2), the depolarization for the 2 mol L$^{-1}$ NMA solutions increasingly deviates from the aqueous case when denaturants such as KI and KSCN are added. For the strongest denaturant of the present study, KSCN, $\Delta\varepsilon$ is enhanced by approximately 30 % for the NMA/KSCN/$H_2O$ solution compared to the KSCN/$H_2O$ samples. As elaborated before, this enhanced depolarization can be assigned to preferential interactions of the salt with NMA. Hence, our results are indicative of enhanced proximity of $Br^-$, $I^-$, and $SCN^-$ to NMA, in accordance with direct interactions of the denaturing anions with amide groups.

The depolarization, which is directly accessible from the measured spectra and model-independent, gives qualitative insights into the ion–amide interactions. To quantify our observations, we deconstructed the individual contributions of water and NMA to the spectra using a relaxation model. For neat water, two relaxation modes were observed in the frequency range of the present study, namely the collective rotational relaxation of hydrogen-bonded water at approximately 20 GHz and a weak relaxation at about 200 GHz.[22] The addition of dipolar NMA molecules has been shown to result in an additional Debye-type relaxation mode at approximately 4 GHz.[20,31] Hence, assuming uncorrelated

  

dipole rotation, we used a combination of three relaxation modes to model the experimental spectra:

$$\hat{\varepsilon}(\nu) = \frac{S_{\mathrm{NMA}}}{1+(2\pi i\nu\tau_{\mathrm{NMA}})} + \frac{S_{\mathrm{water,\,exp}}}{1+(2\pi i\nu\tau_{\mathrm{water}})^{(1-\alpha)}} + \frac{S_{\mathrm{fast}}}{1+(2\pi i\nu\tau_{\mathrm{fast}})} + \varepsilon_\infty + \frac{\kappa}{2\pi i\nu\varepsilon_0} \quad (1)$$

$S_j$ and $\tau_j$ are the relaxation amplitudes and times, respectively, $\varepsilon_\infty$ is the infinite-frequency permittivity, and $\varepsilon_0$ is the permittivity of free space. The last term of Eq. (1) accounts for Ohmic losses that are due to the DC conductivity of the sample, $\kappa$. In analogy to the observations made for many aqueous electrolytes, we used a symmetrically broadened Cole–Cole mode for the main water relaxation with $\alpha$ being a measure for the width of the relaxation mode.[20,32]

Owing to the strongly overlapping relaxation modes of NMA and water, we constrained the description by reducing the number of adjustable parameters. As water is the dominant species in solution ($c_{H_2O}$ is at least 20 times higher than the NMA concentration), the amplitude of the water relaxation was fixed to that of an ideal solution (random ion distribution in solution; for details see the Supporting Information and Refs. [20,28]).

As can be seen from Figure 1 (see also Figure S1), such a constrained model describes the experimental spectra very well. These fits show that the fast water relaxation mode is hardly affected by the addition of salt (see Figures S5 and S6), and only $S_{\mathrm{fast}}$ slightly increases with increasing $c_{\mathrm{salt}}$. This mode can be interpreted in terms of the rapid, small angular motion of a water molecule preceding slower, large angular jumps.[33] As such, the increasing amplitude is consistent with an increasing angular degree of freedom in the hydration shell of the anion.[34] In line with what has been found for binary aqueous electrolytes,[30] $\tau_{\mathrm{water}}$ broadens (Figure S7) and decreases with increasing $c_{\mathrm{salt}}$ (Figure S6), which indicates an on-average broader distribution and weakening of the hydrogen bonds of water[30,35] or analogously a reduced collectivity of the water rotation.[27] Conversely, $\tau_{\mathrm{NMA}}$ increases with increasing $c_{\mathrm{salt}}$, which is in accordance with increasing sample viscosity and thus hydrodynamically controlled rotational motion of the NMA molecules.[20,31] More importantly, the obtained $S_{\mathrm{NMA}}$ values can be directly related to the apparent NMA concentration, that is, the molecules that are not affected by the salt, $c_{\mathrm{NMA,free}}$ (see the Supporting Information). As can be seen from these values in Figure 3, the rotational mobility of NMA is virtually unaffected by the addition of KCl and $KNO_3$. In contrast, KSCN, KI, and KBr markedly reduce $c_{\mathrm{NMA,free}}$, which is in line with the qualitative conclusions from Figure 2 (see above). The observed reduction of $c_{\mathrm{NMA,free}}$ may stem from both the reduced mobility of individual NMA molecules and reduced interactions between NMA molecules.[27]

Following our study on cations,[20] we quantified this interaction assuming an association equilibrium of $n$ NMA molecules interacting with an anion $A^-$ [Eq. (2)], with the corresponding equilibrium constant $K$ defined as Eq. (3).

$$A^- + n\,\mathrm{NMA} \rightleftharpoons n\,\mathrm{NMA}\cdot A^- \quad (2)$$

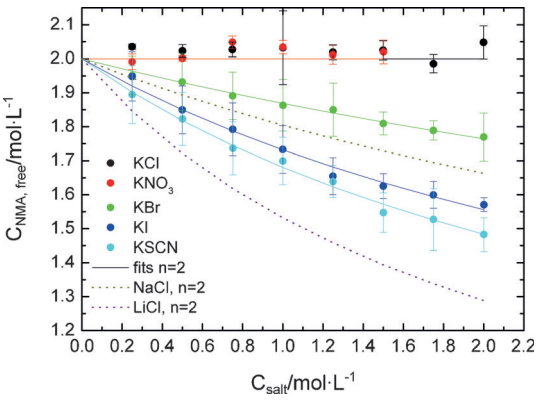


***Figure 3.*** Concentration of free NMA molecules as a function of the salt concentration. The solid lines correspond to fits obtained with Eq. (3) and $n = 2$. Error bars correspond to the standard deviation of at least six independent measurements. For comparison, results for different cations (NaCl and LiCl) with $n = 2$ are included.[20]

$$K = \frac{c_{n\,\mathrm{NMA}\cdot A^-}}{(c_{\mathrm{NMA,free}})^n\, c_{A^-}} \quad (3)$$

As can be seen from the solid lines in Figure 3, such association equilibria excellently describe the observed decrease in $c_{\mathrm{NMA,free}}$ with $c_{\mathrm{salt}}$ assuming the binding of up to two NMA molecules [$n = 2$ in Eq. (3)], whereas $n = 1$ gives a worse description of the data (Figure S8).[36] The association constants thus obtained for $n = 2$ are in line with what one would expect from the Hofmeister series: $K^{\mathrm{DRS}}_{\mathrm{KBr}} = 0.02\ \mathrm{L^2\,mol^{-2}}$, $K^{\mathrm{DRS}}_{\mathrm{KI}} = 0.05\ \mathrm{L^2\,mol^{-2}}$, and $K^{\mathrm{DRS}}_{\mathrm{KSCN}} = 0.07\ \mathrm{L^2\,mol^{-2}}$. For anions with high denaturation efficiencies, such as $SCN^-$ and $I^-$, the $K$ values extracted assuming $n = 1$ (following Ref. [11]) in Eq. (3) ($K^{\mathrm{DRS}}_{\mathrm{KSCN}} = 0.25\ \mathrm{L\,mol^{-1}}$ and $K^{\mathrm{DRS}}_{\mathrm{KI}} = 0.20\ \mathrm{L\,mol^{-1}}$), are lower than those reported using the solubility of amide-rich polymers ($K^{\mathrm{sol}}_{\mathrm{SCN^-}} = 4\ \mathrm{L\,mol^{-1}}$ and $K^{\mathrm{sol}}_{\mathrm{I^-}} = 1.5\ \mathrm{L\,mol^{-1}}$)[11] or the NMR chemical shifts of the amide protons ($K^{\mathrm{NMR}}_{\mathrm{SCN^-}} = 14\ \mathrm{L\,mol^{-1}}$ and $K^{\mathrm{NMR}}_{\mathrm{I^-}} = 3.8\ \mathrm{L\,mol^{-1}}$).[11] This range of inferred interaction strengths highlights the technique dependence of the precise values for the inferred association constants.

The equal sensitivity of the rotational mobility of NMA to interactions with anions and cations allows for a quantitative comparison of the present results to our earlier results on Hofmeister cations.[20] This comparison shows that the anion–amide interaction is weaker than cation–amide binding: As can be seen from the dotted lines in Figure 3, showing $c_{\mathrm{NMA,free}}$ for varying concentrations of NaCl and LiCl, the strongly denaturing $Li^+$ cation has an even larger effect on the mobility of NMA than $SCN^-$. Our results indicate that when comparing monovalent anions and cations located at the very extreme positions in the Hofmeister series, cations can reduce the rotational mobility about twice more than anions ($K^{\mathrm{DRS}}_{\mathrm{KSCN}} = 0.07\ \mathrm{L^2\,mol^{-2}}$ and $K^{\mathrm{DRS}}_{\mathrm{LiCl}} = 0.13\ \mathrm{L^2\,mol^{-2}}$ [20] for $n = 2$).

The observation that the interactions of cations with the NMA C=O group are stronger than those of anions with the N–H group is in accordance with results from molecular dynamics simulations.[9,19] Given that intramolecular amide–

  

amide N–H···O=C hydrogen bonds are a key binding motif that stabilizes the secondary structure of proteins, it might be expected from the ion–amide interaction strengths that cations more strongly destabilize proteins than anions. Yet, anions are overall appreciably more efficient in disrupting the structure of proteins.[2] This apparent contradiction indicates that the interactions of ions with protein amide moieties, which cause a weakening of the amide–amide bonds, are not the only cause of ion-induced protein destabilization. In particular for the anions, additional sites of interaction are the side chains of the amino acids, which are important for determining the protein structure. The destabilizing effect of anions on hydrophobic interactions[37] may explain the disproportionally large effect of anions on protein stability. The observation that the anion–amide interaction strength follows the Hofmeister series indicates that direct ion–amide interactions are also relevant for protein stability, in particular for the stabilization of unfolded (random-coil) proteins in solution with their amide groups exposed to the salt solution.

## Acknowledgements

This work was funded by the Deutsche Forschungsgemeinschaft (DFG, HU1860/4). H.K. acknowledges funding from the European Union's Horizon 2020 Programme (658467).

**Keywords:** amides · anions · denaturation · dielectric spectroscopy · specific ion effects

**How to cite:** *Angew. Chem. Int. Ed.* **2016**, *55*, 8125–8128
*Angew. Chem.* **2016**, *128*, 8257–8261

[1] F. Hofmeister, *Arch. Exp. Pathol. Pharmakol.* **1888**, *24*, 247–260.
[2] Y. Zhang, P. S. Cremer, *Annu. Rev. Phys. Chem.* **2010**, *61*, 63–83.
[3] P. Jungwirth, P. S. Cremer, *Nat. Chem.* **2014**, *6*, 261–263.
[4] W. J. Xie, Y. Q. Gao, *J. Phys. Chem. Lett.* **2013**, *4*, 4247–4252.
[5] A. Salis, B. W. Ninham, *Chem. Soc. Rev.* **2014**, *43*, 7358–7377.
[6] J. Holzmann, R. Ludwig, A. Geiger, D. Paschek, *Angew. Chem. Int. Ed.* **2007**, *46*, 8907–8911; *Angew. Chem.* **2007**, *119*, 9065–9069.
[7] D. Paschek, R. Ludwig, *Angew. Chem. Int. Ed.* **2011**, *50*, 352–353; *Angew. Chem.* **2011**, *123*, 368–370.
[8] Y. Marcus, *Chem. Rev.* **2009**, *109*, 1346–1370.
[9] a) J. Hladílková, J. Heyda, K. B. Rembert, H. I. Okur, Y. Kurra, W. R. Liu, C. Hilty, P. S. Cremer, P. Jungwirth, *J. Phys. Chem. Lett.* **2013**, *4*, 4069–4073; b) J. Paterová, K. B. Rembert, J. Heyda, Y. Kurra, H. I. Okur, W. R. Liu, C. Hilty, P. S. Cremer, P. Jungwirth, *J. Phys. Chem. B* **2013**, *117*, 8150–8158.
[10] H. Meuzelaar, M. R. Panman, S. Woutersen, *Angew. Chem. Int. Ed.* **2015**, *54*, 15255–15259; *Angew. Chem.* **2015**, *127*, 15470–15474.
[11] K. B. Rembert, H. I. Okur, C. Hilty, P. S. Cremer, *Langmuir* **2015**, *31*, 3459–3464.
[12] K. B. Rembert, J. Paterová, J. Heyda, C. Hilty, P. Jungwirth, P. S. Cremer, *J. Am. Chem. Soc.* **2012**, *134*, 10039–10046.
[13] H. Kim, H. Lee, G. Lee, H. Kim, M. Cho, *J. Chem. Phys.* **2012**, *136*, 124501.
[14] H. I. Okur, J. Kherb, P. S. Cremer, *J. Am. Chem. Soc.* **2013**, *135*, 5062–5067.
[15] R. L. Baldwin, *Biophys. J.* **1996**, *71*, 2056–2063.
[16] E. A. Algaer, N. F. A. van der Vegt, *J. Phys. Chem. B* **2011**, *115*, 13781–13787.
[17] C. P. Rao, P. Balaram, C. N. R. Rao, *J. Chem. Soc. Faraday Trans. 1* **1980**, *76*, 1008–1013.
[18] N. Schwierz, D. Horinek, R. R. Netz, *Langmuir* **2013**, *29*, 2602–2614.
[19] a) H. Du, R. Wickramasinghe, X. Qian, *J. Phys. Chem. B* **2010**, *114*, 16594–16604; b) J. Heyda, J. C. Vincent, D. J. Tobias, J. Dzubiella, P. Jungwirth, *J. Phys. Chem. B* **2010**, *114*, 1213–1220.
[20] a) V. Balos, M. Bonn, J. Hunger, *Phys. Chem. Chem. Phys.* **2015**, *17*, 28539–28543; b) V. Balos, M. Bonn, J. Hunger, *Phys. Chem. Chem. Phys.* **2016**, *18*, 1346–1347.
[21] a) F. Kremer, A. Schönhals, *Broadband Dielectric Spectroscopy*, Springer, Berlin, **2003**; b) U. Kaatze, Y. Feldman, *Meas. Sci. Technol.* **2006**, *17*, R17–R35.
[22] T. Fukasawa, T. Sato, J. Watanabe, Y. Hama, W. Kunz, R. Buchner, *Phys. Rev. Lett.* **2005**, *95*, 197802.
[23] W. Ensing, J. Hunger, N. Ottosson, H. J. Bakker, *J. Phys. Chem. C* **2013**, *117*, 12930–12935.
[24] R. Pottel, D. Adolph, U. Kaatze, *Ber. Bunsenges. Phys. Chem.* **1975**, *79*, 278–285.
[25] M. Sega, S. Kantorovich, A. Arnold, *Phys. Chem. Chem. Phys.* **2015**, *17*, 130–133.
[26] N. Ottosson, J. Hunger, H. J. Bakker, *J. Am. Chem. Soc.* **2014**, *136*, 12808–12811.
[27] K. F. Rinne, S. Gekle, R. R. Netz, *J. Phys. Chem. A* **2014**, *118*, 11667–11677.
[28] Note that for $KNO_3$, the magnitude of $\Delta\varepsilon$ is slightly smaller than what would be expected assuming KD and dilution, which can be explained by the weak formation of dipolar ion pairs (see Figures S3 and S4). Similiarly, for KSCN, the non-centrosymmetric nature of $SCN^-$ results in a weak contribution of the rotation of $SCN^-$ to the spectra. These weak contributions to the spectra were corrected for in our quantitative analysis (see the Supporting Information).
[29] T. Chen, G. Hefter, R. Buchner, *J. Phys. Chem. A* **2003**, *107*, 4025–4031.
[30] W. Wachter, W. Kunz, R. Buchner, G. Hefter, *J. Phys. Chem. A* **2005**, *109*, 8675–8683.
[31] U. Kaatze, H. Gerke, R. Pottel, *J. Phys. Chem.* **1986**, *90*, 5464–5469.
[32] U. Kaatze, *J. Phys. Chem.* **1987**, *91*, 3111–3113.
[33] A. Y. Zasetsky, *Phys. Rev. Lett.* **2011**, *107*, 117601.
[34] S. T. van der Post, K. Tielrooij, J. Hunger, E. H. G. Backus, H. J. Bakker, *Faraday Discuss.* **2013**, *160*, 171.
[35] H. J. Bakker, *Chem. Rev.* **2008**, *108*, 1456–1473.
[36] With $n$ as a free parameter, values scattered around $n = 2$ were obtained: $n_{KBr} = (2.6 \pm 0.7)$, $n_{KI} = (2.0 \pm 0.5)$, and $n_{KSCN} = (1.8 \pm 0.4)$.
[37] P. Jungwirth, B. Winter, *Annu. Rev. Phys. Chem.* **2008**, *59*, 343–366.

Received: March 19, 2016
Published online: May 30, 2016

  